



# HHS Public Access

Author manuscript

*J Leukoc Biol.* Author manuscript; available in PMC 2019 June 01.

Published in final edited form as:

*J Leukoc Biol.* 2018 December ; 104(6): 1253–1261. doi:10.1002/JLB.5TA0318-110RRR.

## Progressive mechanical confinement of chemotactic neutrophils induces arrest, oscillations, and retrotaxis

Xiao Wang<sup>1</sup>, Emily Jodoin<sup>1</sup>, Julianne Jorgensen<sup>1</sup>, Jarone Lee<sup>2</sup>, James J. Markmann<sup>3</sup>, Sule Cataltepe<sup>4</sup>, and Daniel Irimia<sup>1</sup>

<sup>1</sup>Department of Surgery, BioMEMS Resource Center, Massachusetts General Hospital, Harvard Medical School, Shriners Burns Hospital, Boston, Massachusetts, USA

<sup>2</sup>Department of Emergency Medicine, Massachusetts General Hospital, Harvard Medical School, Boston, Massachusetts, USA

<sup>3</sup>Department of Newborn Medicine, Brigham and Women's Hospital, Harvard Medical School, Boston, Massachusetts, USA

<sup>4</sup>Division of Transplantation, Department of Surgery, Massachusetts General Hospital, Harvard Medical School, Boston, Massachusetts, USA

### Abstract

Neutrophils reach the sites of inflammation and infection in a timely manner by navigating efficiently through mechanically complex interstitial spaces, following the guidance of chemical gradients. However, our understanding of how neutrophils that follow chemical cues overcome mechanical obstacles in their path is restricted by the limitations of current experimental systems. Observations in vivo provide limited insights due to the complexity of the tissue environment. Here, we developed microfluidic devices to study the effect of progressive mechanical confinement on the migration patterns of human neutrophils toward chemical attractants. Using these devices, we identified four migration patterns: arrest, oscillation, retrotaxis, and persistent migration. The proportion of these migration patterns is different in patients receiving immunosuppressant treatments after kidney transplant, patients in critical care, and neonatal patients with infections and is distinct from that in healthy donors. The occurrence of these migration patterns is independent of the nuclear lobe number of the neutrophils and depends on the integrity of their cytoskeletal components. Our study highlights the important role of mechanical cues in moving neutrophils and suggests the mechanical constriction-induced migration patterns as potential markers for infection and inflammation.

---

**Correspondence** Daniel Irimia, BioMEMS Resource Center, Division of Surgery, Innovation and Bioengineering, Department of Surgery, Massachusetts General Hospital, Harvard Medical School, Shriners Burns Hospital, MGH-CNY, 114 16th St., #1404 Boston, MA 02129, USA. [dirimia@mgh.harvard.edu](mailto:dirimia@mgh.harvard.edu).

#### AUTHORSHIP

X.W. and D.I. designed research; X.W., E.J., and J.J. performed research and analyzed the data; X.W., J.L., S.C., J.F.M., and D.I. wrote the paper.

#### SUPPORTING INFORMATION

Additional information may be found online in the Supporting Information section at the end of the article.

#### DISCLOSURES

The authors declare no conflicts of interest.

## Keywords

diagnosis of infection and inflammation; microfluidic assay; neutrophil chemotaxis

---

## 1 | INTRODUCTION

Cell migration is essential in a variety of physiological processes, such as immune responses<sup>1,2</sup> and wound healing,<sup>3,4</sup> as well as diseases such as cancer invasion and metastasis.<sup>5,6</sup> Motile cells integrate and prioritize surrounding chemical and physical cues to navigate through complex intercellular and interstitial spaces. Neutrophils are fast-migrating immune cells serving as the first line of host defense against tissue injury and infection.<sup>2</sup> Upon tissue injury, neutrophils in peripheral blood rapidly breach through endothelial cell lining and interstitial spaces to the injured sites to eliminate pathogens and mediate downstream immune responses.<sup>7</sup> The chemotaxis of neutrophils and other immune cells not only depends on their ability to sense and prioritize chemical cues<sup>8</sup> but also relies on their responses to complex extracellular mechanical confinement.<sup>9</sup> Although the chemotaxis of neutrophils has been extensively studied, how mechanical cues affect their migration in chemotaxis is not fully investigated yet.

Microfluidics is a powerful technology which provides the ability to study single cells in engineered microchannels with high temporal and spatial resolutions.<sup>10,11</sup> Exploiting microfluidics in the study of chemotaxis has advanced our understanding in leukocyte trafficking in the context of homeostasis and diseases and offered new opportunities in clinical diagnostics and therapeutic development.<sup>8,12–17</sup> The study of neutrophil chemotaxis using microfluidic assays predominately focuses on probing the motility parameters such as velocity, directionality, and migration trajectories of chemotactic cells, however few investigated how mechanical cues can potentially affect neutrophil migration during chemotaxis.

Here, we investigate the effect of progressive mechanical confinement on the chemotaxis of human neutrophils. For this study, we designed a microfluidic device comprised of a large array of microchannels with a tapered geometry (Fig. 1). We found the progressive mechanical confinement induces arrest, oscillation, and retro-taxis migration patterns. We employed the tapered channel assay to measure the migration patterns of neutrophils from organ-transplant patients receiving immune-suppressing treatments as well as from adult and neonatal patients with infections. We found that the migration patterns of the patient neutrophils were significantly altered and included larger proportion of arrest, oscillation, and retrotaxis than the healthy individuals. Moreover, these patterns are independent on the number of nuclear lobes and depend on the types of the chemokine and the cytoskeletal integrity of the neutrophils. Our study emphasizes the importance of mechanical cues in neutrophil chemotaxis and highlights the potential of the mechanically induced migration patterns as novel markers for monitoring neutrophil alterations during infection and inflammatory conditions.

## 2 | MATERIALS AND METHODS

### 2.1 | Device fabrication

The microfluidic devices were fabricated using standard soft lithography. First, we fabricated the two-layer master mold in negative photoresist (SU-8, Microchem, Newton, MA) on a 4-inch silicon wafer. The first layer was 2  $\mu\text{m}$  thin containing the patterns of the tapered migration channels (Supplementary Fig. 1A, blue layer). The second layer was 75  $\mu\text{m}$  thick and consists of cell-loading channels (CLC) and chemokine chambers (Supplementary Fig. 1A, red layer). A ratio of 10:1 PDMS base and curing agent were mixed, cast on the master mold, and degassed thoroughly (PDMS, Sylgard, 184, Elsworth Adhesives, Wilmington, MA). We transferred the wafer into an oven at 65°C to cure overnight. After curing, we peeled off the PDMS layer from the wafer and cut out individual devices using a scalpel. We punched the inlets and outlets of the devices using a 0.75 mm diameter biopsy puncher (Harris Uni-Core, Ted Pella) and irreversibly bonded them to a glass-bottom multiwell plate (MatTek Co., Ashland, MA).

### 2.2 | Neutrophil isolation

Human blood samples from healthy donors (aged 18 years and older) were purchased from Research Blood Components, LLC. All blood specimens from patients were obtained with informed consent. Human neutrophils were isolated within 2h after drawn using the human neutrophil direct isolation kit (STEMcell Technologies, Vancouver, Canada) following the manufacturer's protocol. After isolation, neutrophils were stained with Hoechst 33342 trihydrochloride dye (Life Technologies). Stained neutrophils were then suspended in Iscove's Modified Dulbecco's Medium (IMDM) containing 20% FBS (Thermo Fisher Scientific) at a concentration of  $2 \times 10^7$  cells  $\text{ml}^{-1}$ .

Blood from organ transplant and intensive care unit (ICU) patients was collected from patients after informed consent and following a protocol approved by the institutional review board at the Massachusetts General Hospital. Tracheal aspirate fluid (TAF) from neonatal patients was collected as discarded samples from patients as part of normal medical care and following a protocol approved by the institutional review board at the Brigham and Women Hospital. Neutrophils from organ transplant, ICU patients, and neonatal intensive care units (NICU) patients were isolated using the same protocol. Neonatal TAF neutrophils were prepared by directly re-suspending neutrophils in IMDM containing 20% FBS. For disruption of contractility or microtubule dynamics, we incubated isolated neutrophils with blebbistatin or nocodazole, respectively at 50  $\mu\text{M}$  for 30 min, before loading into the chip.

### 2.3 | Device operation and imaging

fMLP (Sigma-Aldrich) and LTB4 (Cayman Chemical, Ann Arbor, Michigan, USA) were diluted in IMDM containing 20% FBS to working concentrations with 100 nM fibronectin (R&D systems, Inc.). Ten microliters of the chemokine solution was pipetted into each device. The well plate was then placed in a desiccator under vacuum for 10 min. The well plate was then taken out from the desiccator for 15 min until the devices were filled completely with the solution. Three milliliters of media (IMDM + 20% FBS) was then added to each well to cover the devices. Each device was then washed by pipetting 10  $\mu\text{l}$

media through the inlet. Finally, 2  $\mu\text{L}$  neutrophil suspension was pipetted into each device. Time-lapse images of neutrophil migration were captured at 10 $\times$  or 20 $\times$  magnification using a fully automated Nikon TiE microscope (Micro Device Instruments). The microscope is equipped with a biochamber heated at 37°C and 5% CO<sub>2</sub>.

#### 2.4 | Analysis of neutrophil migration

We used Trackmate module in Fiji ImageJ (ImageJ, NIH) to track and analyze cell trajectories automatically. We identified four migration behaviors including persistent migration (P), arrest (A), oscillation(O), and retrotaxis (R). Persistent migration indicates neutrophils that migrated through the channels without changing directions. Arrest describes neutrophils that are trapped in the channels. Oscillation indicates neutrophils that change migration direction more than two times. Retrotaxis describes neutrophils that migrated back to the cell-loading channel.

#### 2.5 | Statistical analysis

Statistical significance of the differences between multiple data groups were tested using one-way Analysis of Variance (ANOVA) in GraphPad Prism (GraphPad Software). Within ANOVA, significance between two sets of data was further analyzed using two-tailed *t*-tests. All the box plots consist of a median line, the mean value (the cross), and whiskers from minimum value to maximum value.

### 3 | RESULTS

#### 3.1 | The Microfluidic device to study neutrophil chemotaxis during progressive mechanical confinement

Our microfluidic device consists of an array of 756 tapered channels, with cross-section starting at 20  $\mu\text{m}^2$  (10  $\mu\text{m} \times 2 \mu\text{m}$ , width  $\times$  height) and decreasing to 6  $\mu\text{m}^2$  (Supplementary Fig. S1). The migration channels are 500  $\mu\text{m}$  in length and connect one shared cell-loading channel to multiple chemoattractant chambers (ICCs) (Supplementary Fig. S1A–C). A chemoattractant gradient is established along the migration channels, from CLCs to ICCs (Supplementary Fig. S1D and E). This design enables us to investigate neutrophil chemotaxis in conditions of progressive mechanical confinement and make direct comparison to the migration of neutrophils inside channels of uniform cross-section. We employed time-lapse imaging and automatic cell tracking to investigate the active deformation and migration patterns of single neutrophils with high spatial and temporal resolutions (Supplementary Fig. S1F and G).

#### 3.2 | Progressive mechanical constriction of chemotactic neutrophils induces three additional migration patterns

We compared human-neutrophil migration patterns in uniform and tapered microchannels (Fig. 1A). Neutrophils in uniform channels with a cross-section of 20  $\mu\text{m}^2$  migrated persistently in fMLP, LTB<sub>4</sub>, and IL8 gradients (Fig. 1C–D). We found that tight mechanical constriction in the tapered microchannel induced three additional migration patterns which are rarely seen in the uniform channel including arrest (A), oscillation (O), and retrotaxis (R) (Fig. 1B–D, and Supplementary video). The total percentages of A, O, and R patterns in the

tapered microchannels in fMLP, LTB4, and IL8 gradients are 15, 24, and 29%, respectively (Fig. 1D). We found that the pattern of the migration patterns in the tapered microchannels is chemokine-dependent. 84, 76, and 70% neutrophils migrated persistently in fMLP, LTB4, and IL8 gradient, respectively (Fig. 1C). In fMLP gradient, 7% and 7% neutrophils showed arrest and retrotaxis and only 2% showed oscillation. In contrast, 18% neutrophils exhibited oscillation in the LTB4 gradient and 23% neutrophils exhibited retrotaxis in the IL8 gradient.

The tapered microchannels enable precise measurements of the critical cross-section (CCS) at which A, O, and R patterns occur (Fig. 1E and F). The results show that the average CCSs are at 10.5, 9.2, and 10  $\mu\text{m}^2$  in fMLP, LTB4, and IL8 gradients, respectively (Fig. 1E). And the cross-sections are more dispersed in fMLP and IL8 gradients than LTB4 gradient. The histograms of CCSs further show that 90% of A, R, and O patterns occur only at a cross-section of  $<14 \mu\text{m}^2$ . The distributions of CCSs are skewed toward the right for all chemoattractants, peaking at 6~8  $\mu\text{m}^2$  in fMLP and IL8 gradients and 8~10  $\mu\text{m}^2$  in LTB4 gradient (Fig. 1F). Taken together, our results indicate that the mechanical constriction in channels can interfere with the neutrophil responses to chemical gradients and alter the migration of neutrophils.

### 3.3 | Morphological changes induced by mechanical constriction in chemotactic neutrophils

We investigated the morphology of the neutrophils from healthy individuals during migration through tapered microchannels. Migrating neutrophils showed a typical broad leading edge toward the chemokine and a rounded uropod at the rear (Fig. 2A, yellow and green arrows). As they confront tightening mechanical constriction, the length of the cell, the relative location of the nucleus, and the arrangement of the nuclear lobes gradually transformed to adapt to the changing physical environment. Neutrophils gradually elongated from ~25 to ~70  $\mu\text{m}$  when advancing into the narrowing channel (Fig. 2B), while their total volume remained relatively constant (Supplementary Fig. S2). In addition, the center of the nucleus gradually shifted toward the rear of the cell. The distance from the center of the nucleus to the center of the cell increased from ~5 to ~15  $\mu\text{m}$  (Fig. 2C).

### 3.4 | Nuclear lobe re-arrangement induced by mechanical constriction during neutrophil chemotaxis

We observed that neutrophils chemotaxing through tapered channels progressively re-arranged their nuclear lobes from a cluster into a string in the decreasing cross-section (Fig. 2A). Such transformation happens in all the neutrophils, independent of the number of lobes (Supplementary Fig. S3) leading to an increase of nuclear aspect ratio from 1 (cluster) to 7 (string) (Fig. 2D). We measured the average cross-section of the cluster-string transformation to be ~9.5  $\mu\text{m}^2$  and independent of chemokine types (Fig. 2E). Furthermore, we found that the average cross-section decreases with increasing number of lobes (Fig. 2F and G). Neutrophils with 3, 4, and 5 lobes undergo the cluster-string transformation at average cross-sections of 10.1, 9.5, and 8.0  $\mu\text{m}^2$  in fMLP gradient and 10.3, 9.1, and 8.6  $\mu\text{m}^2$  in LTB4 gradient. Finally, we estimated the volume of the neutrophil nuclei by taking advantage of the constant, known height of the channels that compresses the nucleus to a

uniform thickness. From the measurements of the area of the nuclei in the horizontal plane and the height of the channels, we calculated that while the nuclei of neutrophils with different lobe numbers have a similar volume, the size and volume of individual lobes is negatively correlated to the number of lobes. The total volume of the nucleus is  $\sim 110 \mu\text{m}^3$  (Fig. 2I), while the average volume of individual lobes is 35, 29, and  $19 \mu\text{m}^3$  for 3, 4, and 5-lobe neutrophils, correspondingly (Fig. 2H).

We also investigated whether the number of neutrophil nuclear lobes correlates with the migration patterns in response to mechanical constrictions (Fig. 3). We hypothesized that neutrophils with more lobes migrate through smaller space without arrest, retrotaxis, or oscillation, due to the flexibility of arrangement the lobes and smaller lobe volume. Surprisingly, we found that neutrophils with 3–5 lobes exhibited similar migration patterns over the entire range of cross-sections tested. We measured a percentage of 80% neutrophils migrating through tapered channels in a gradient of fMLP, regardless of the number of their lobes (Fig. 3A and B). We also studied whether, among the neutrophils arrested inside the channels, those with more lobes can migrate deeper (Fig. 3C). We found that the cross-section at which neutrophils are arrested is  $\sim 10 \mu\text{m}^2$  and independent of the number of lobes (Fig. 3C). Overall, our results suggest that the number of lobes, in the 3–5 range is not correlated with the neutrophil responses to the mechanical constriction in the tested range of cross-section.

### 3.5 | The effects of cytoskeleton on mechanically induced migration patterns

We explored the effects of myosin II-mediated contractility and microtubule network on the migration patterns. Inhibiting myosin II-mediated contractility increased the percentage of arrest from 7 to 30%, while decreasing the percentage of persistent migration from 84 to 57% (Fig. 3D). Several blebbistatin-treated neutrophils showed elongated morphology (Supplementary video). Strikingly, after being arrested, the leading edge of the neutrophil extended for  $250 \mu\text{m}$  into the chemoattractant chamber. Interfering with the microtubule stability dramatically increases the proportion of oscillatory pattern, from 1.7 to 50% (Fig. 3D, Supplementary video). The percentage of persistent migration decreases from 84 to 36%. Treating neutrophils with both inhibitors further impairs the migration. The percentage of persistent migration decreases to 25%. The percentage of arrest increases to 52%, higher than that for neutrophils treated with blebbistatin only. The proportion of oscillatory pattern is roughly 10 times larger than in untreated controls. The critical cross-section for the occurrence of AOR patterns is in a range of  $6\text{--}14 \mu\text{m}$ , with an average of  $10 \mu\text{m}$ , similar to the control (Fig. 3E). The histogram of the critical cross-section shows that  $>90\%$  of A, R, and O patterns occurred at a cross-section range of  $<14 \mu\text{m}^2$ . Taken together, our results show that both myosin II contractility and microtubule dynamics contribute to neutrophil migration under progressive mechanical confinement conditions (Fig. 3F).

### 3.6 | Neutrophils from patients exhibit distinct migration patterns

We studied the migration patterns of neutrophils from organ transplant patients receiving immune-suppressing treatments, from patients in intensive care units, and from TAF from neonates. We found neutrophils from patients often exhibit migration patterns that are distinct from those of healthy controls (Fig. 4). The most affected neutrophils were those

from patients with infections (neonates and ICU). In transplant patients receiving immunosuppressive therapy, the migration patterns were also altered.

Patients with organ transplant receive immune-suppressive therapies to prevent allograft rejection. We studied the patterns of neutrophil migration and found suppressed persistent migration pattern of neutrophils in blood samples from 62% of patients. The persistent migration pattern of neutrophils from three out of eight patients was similar to or higher than the healthy control. Kidney biopsy from patient 6 showed borderline changes suspicious for acute graft rejection, and thrombotic microangiopathy and acute tubular injury, for patients 8 and 3, respectively. The last two conditions are often described in the literature as a severe complications of kidney transplantation linked to graft failure (Supplementary Table S1). None of the patients presented graft failure during the course of this study.

Some neutrophils from the impacted group displayed an elongated tail in the larger cross-section of the channel (Fig. 4A, green arrows, Supplementary video), and an over-extended leading edge in the smaller cross-section (Fig. 4A, red arrow). These changes in neutrophil morphology were only observed in samples from transplant patients. The neutrophils from these patients are also less capable of migrating through the narrowest section of the channels (Fig. 4C). Our assay further revealed that the proportions of A, O, R patterns are different among these patients. For patient 1 and 2, higher percentage of neutrophils showed arrest pattern. For patient 4, 5, and 7, however, higher percentage of neutrophils exhibited retrotaxis pattern. The average critical cross-section of A, O, and R patterns is  $\sim 10 \mu\text{m}^2$  across all the patients and similar to the control (Fig. 4D).

We tested the neutrophils from patients in intensive care units who had been diagnosed with infections and sepsis (Supplementary Table S2). We observed that the migrating neutrophils from septic patients displayed an olive-shaped morphology, with a poorly defined leading edge and uropod (Fig. 4B, bright field, Supplementary video). The nucleus of these neutrophils was located arbitrarily in the cells and had abnormal lobe arrangements (Fig. 4B). The cluster-string transformation happened at an average cross-section of  $\sim 15 \mu\text{m}^2$ , which is larger than the healthy control (Supplementary Fig. S4A). The distance between the centers of the nucleus and the cell is  $< 5 \mu\text{m}$  at the entire range of cross-section, which is much smaller than the healthy control (Supplementary Fig. S4B). We found that the migrating neutrophils from ICU patients displayed significantly more A, O, and R patterns than healthy individuals, in the range of 20~40% (Fig. 4C). Less than 25% of neutrophils migrated with persistent migration pattern. For patients 1 and 3, the cross-sections of A, O, and R patterns are  $\sim 14 \mu\text{m}^2$ , which are significantly larger than the healthy control (Fig. 4D). For patient P2, the cross-section is similar to the control, despite higher percentage of A, O, and R patterns. Overall, the migration patterns of neutrophils from ICU patients are distinct from those of healthy individuals and organ transplant patients.

We further studied the changes of neutrophil migration patterns in the ICU patients during treatment. We tested the neutrophils from P1 at Day 1, 6, and 8 during hospitalization (Supplementary Fig. S4C and D). The percentage of neutrophil persistent migration through the narrowest structure of the tapered channels increased from 5, 50 to 93% at Day 1, 6, and 8, respectively. At Day 8, the percentages of A, O, and R were restored to the levels of

healthy controls. The critical cross-section decreased from an average of 14 to 10  $\mu\text{m}^2$  at Day 8, consistent with the recovery of the neutrophil migration patterns.

We studied neutrophils from TAF of neonates in neonatal intensive care units. These infants were under mechanical ventilation and were susceptible to ventilator-associated pneumonia (VAP).<sup>18</sup> Different from other patient samples, 60~92% neonatal TAF neutrophils exhibited arrest pattern (Fig. 4C and D). The critical occurrence cross-sections of A, O, and R patterns are predominately from 16 to 18  $\mu\text{m}^2$ , which are larger than adult healthy control and neutrophils from other adult patients.

## 4 | DISCUSSION

We investigated the impact of mechanical constrictions on neutrophil migratory behavior during chemotaxis through tapered channels in microfluidic devices. We found that arrest, oscillation, and retrotaxis patterns are induced during the chemotaxis of human neutrophils in conditions of progressive mechanical confinement. We also found that the proportion of these patterns was distinct between healthy individuals and patients. These migration patterns are concealed when using large channels or flat surfaces and are only revealed by the tight mechanical confinement. For example, our previous work showed that in 36  $\mu\text{m}^2$  microchannels, ~100% human neutrophils from healthy donors migrated persistently, without changing directions in both LTB<sub>4</sub> and fMLP gradients.<sup>8</sup> Others have taken advantage of the persistent migration of HL60 neutrophil-like leukemia cells to study the protrusive behavior within confined spaces.<sup>19</sup> One should note that in a channel with a cross-section below a certain threshold, chemotaxing neutrophils can temporarily plug the channel.<sup>19</sup> Consequently, chemokine molecules would be enriched in the cell front and diluted in the cell rear, leading to a local gradient sharper than that in the absence of the neutrophil. One would expect persistent migration in smaller channels due to the sharper gradient. However, the fact that we observed non-persistent migration patterns indicates the important role of tight mechanical confinement in guiding the migration of neutrophils.

Arrest, oscillation, and reverse migration patterns of chemotactic neutrophils have been observed in both in vivo and in vitro models.<sup>13,20–23</sup> However, the role of mechanical confinements in inducing these patterns was underappreciated due to the geometrical complexity of the in vivo environments and the limitations of in vitro 3D gel matrixes. Our device provides a consistent and broad range of mechanical confinement to each neutrophil and enables us to map the migratory responses of a large population of neutrophils to mechanical cues with greater parametric details than any previous studies. Our measurements show that the patterns of migration in narrow channels depend on the types of chemokines. The differences of the migration patterns among these chemokines only emerge at a cross-sections less than 14  $\mu\text{m}^2$ . Combined, these results suggest the tight mechanical environment competes with the chemokine gradient and has a dominant impact on the migration behavior of neutrophils during chemo-taxis.

We took advantage of the engineered microchannels and quantified the process of neutrophil nuclear lobes unfolding and found the average cross-section of the cluster-string transformation to be ~10  $\mu\text{m}^2$ . This transformation was independent of chemokines and



negatively correlated with the number of lobes, and consistent with the results of previous neutrophil migration studies in 3D collagen matrix.<sup>21</sup> Whether the transformation is an active process of neutrophils or a passive process solely driven by mechanical constriction is still unknown. Future studies, by passively flowing non-activated neutrophils through the channel and observing the dynamic arrangement of nuclear lobes, may provide further insights in this process. A recent study<sup>24</sup> suggested that nuclear envelope composition, instead of nuclear shapes (round or lobulated), determines the active deformability of HL-60 cells migrating through small pores. We further showed that the number of lobes has minimal impact on the ability of neutrophils to migrate through channels with a cross-section as small as  $6 \mu\text{m}^2$ . Whether neutrophil lobes are important to migration in cross-section smaller than  $6 \mu\text{m}^2$  remains unexplored. We can only speculate that neutrophils with more lobes may be more capable of migrating through such small space, due to the smaller size of individual lobes.

Previous studies on leukocyte transmigration using 3D collagen matrix or cultured endothelial monolayers showed that contractility is crucial for leukocyte transmigration through endothelial lining and dense collagen matrix.<sup>21,25,26</sup> Inhibition of contractility reduced the percentage of cells undergoing transmigration and increased the time of transmigration.<sup>25</sup> Our results confirm this finding, showing that four times more neutrophils with inhibited contractility are arrested in the confined space compared to untreated controls. This effect appears to be cross-sectional dependent, with the impact of interfering with Myosin II contractility larger for smaller cross-sections. Furthermore, the increased length of the blebbistatin-treated cells suggests that Myosin II contractility is most important at the back of the moving cells. Our study also confirms the role of microtubules during directional persistent migration, as previously revealed in micropipette tip experiments on 2D surfaces.<sup>27</sup> Our results show that the depolymerization of microtubules increases the proportion of oscillatory migration 30-fold, with the effect more pronounced in the smaller section of the microchannels. Intriguingly, we found that co-treatment with Myosin II and microtubule inhibitors further enhances the arrest of neutrophils in confined space. The increase in arrested migration pattern by the combination treatment is at odds with previous studies showing that microtubule de-polymerization enhances cell contractility through the activation of RhoA and Rho-associated kinase (ROCK).<sup>28-30</sup> We speculate that the increased myosin contractility may be taking place at all locations throughout the moving cells, overall having a detrimental effect on the migration in progressively confined channels. The combination treatment compared to nocodazole alone treatment reduces the ratio of oscillating to persistently migrating neutrophils from 1.4:1 down to 0.7:1 suggesting that the relationship between myosin II and microtubules may be bidirectional and more complex than currently known. Future work studying the localization of myosin and microtubules may provide further insights on the contribution of cytoskeleton to neutrophil migratory behaviors in confined channels.

Previous studies show that neutrophil chemotaxis toward fMLP, LTB<sub>4</sub>, and IL8 is impaired in patients with infections and sepsis.<sup>31-35</sup> As a result, fewer neutrophils arrive at the sites of infection, slowing down pathogen clearance and promoting pathogen spreading. The activated neutrophils further release proteolytic enzymes and oxidants leading to dysfunction and failure of organs.<sup>36</sup> The impairment of chemotaxis in sepsis has been shown to be

caused by the internalization of CXCR2 and high expression of G protein-coupled receptor kinase 2 (GRK2) and GRK5 in septic neutrophils, which desensitizes neutrophils and reduces the chemotaxis to sites of infection.<sup>32,37</sup> In addition to these previous findings, our study discovers that the septic neutrophils might lose cytoskeletal integrity, which dampens their ability to chemotax through tight mechanical environment. This defect could potentially limit directional migration and promote the mechanical arrest of activated neutrophils in endothelial junctions, interstitial space or capillary vessels, causing further tissue damage. Future investigation of patient neutrophils with this precise microfluidic assay may provide novel insights in the pathology of sepsis and inflammatory diseases. With further validation, the assay could also serve as a precise tool for predicting the severity of diseases and developing effective therapeutic intervention.

## Supplementary Material

Refer to Web version on PubMed Central for supplementary material.

## ACKNOWLEDGMENTS

We thank Gur Agci for his help with setting up experiments and data analysis. We also thank Kerry Crisalli, R.N, Carrie Holland, R.N, Vicki Sein, M.D., and Kelsey L. Brait for assistance in recruiting patients. This project was supported by funding from the National Institutes of Health, National Institute of General Medical Sciences (GM092804), National Institute of Allergy and Infectious Diseases (AI113937) and Shriners Burns Hospital. Microfluidic devices were manufactured at the BioMEMS Resource Center at Massachusetts General Hospital, supported by a grant from the National Institute of Biomedical Imaging and Bioengineering (EB002503).

## REFERENCES

1. Weninger W, Biro M, Jain R. Leukocyte migration in the interstitial space of non-lymphoid organs. *Nat Rev Immunol.* 2014;14:232–246. [PubMed: 24603165]
2. Kolaczowska E, Kubes P. Neutrophil recruitment and function in health and inflammation. *Nat Rev Immunol.* 2013;13:159–175. [PubMed: 23435331]
3. De Oliveira S, et al. Neutrophil migration in infection and wound repair: going forward in reverse. *Nat Publ Gr.* 2016;16:378–391.
4. Martin P Wound healing—aiming for perfect skin regeneration. *Science.* 1997;276:75–81. [PubMed: 9082989]
5. Paul CD, Mistriotis P, Konstantopoulos K. Cancer cell motility: lessons from migration in confined spaces. *Nat Rev Cancer.* 2017;17:131–140. [PubMed: 27909339]
6. Gupta GP, Massagué J. Cancer metastasis: building a framework. *Cell.* 2006;127:679–695. [PubMed: 17110329]
7. Van Haastert PJM, Devreotes PN. Chemotaxis: signalling the way forward. *Nat Rev Mol Cell Biol.* 2004;5:626–634. [PubMed: 15366706]
8. Boneschansker L, Yan J, Wong E, Briscoe DM, Irimia D. Microfluidic platform for the quantitative analysis of leukocyte migration signatures. *Nat Commun.* 2014;5:4787. [PubMed: 25183261]
9. Vargas P, Barbier L, Sáez PJ, Piel M. Mechanisms for fast cell migration in complex environments. *Curr Opin Cell Biol.* 2017;48:72–78. [PubMed: 28641118]
10. Whitesides GM. The origins and the future of microfluidics. *Nature.* 2006;442:368–373. [PubMed: 16871203]
11. Sackmann EK, Fulton AL, Beebe DJ. The present and future role of microfluidics in biomedical research. *Nature.* 2014;507:181–189. [PubMed: 24622198]
12. Li Jeon N, Baskaran H, Dertinger SK, Whitesides GM, Van de Water L, Toner M. Neutrophil chemotaxis in linear and complex gradients of interleukin-8 formed in a microfabricated device. *Nat Biotechnol.* 2002;20:826–830. [PubMed: 12091913]

13. Hamza B, Irimia D. Whole blood human neutrophil trafficking in a microfluidic model of infection and inflammation. *Lab Chip*. 2015;15:2625–2633. [PubMed: 25987163]
14. Sackmann EK, Berthier E, Schwantes EA, et al. Characterizing asthma from a drop of blood using neutrophil chemotaxis. *Proc Natl Acad Sci U S A*. 2014;111:5813–5818. [PubMed: 24711384]
15. Jones CN, Moore M, Dimisko L, et al. Spontaneous neutrophil migration patterns during sepsis after major burns. *PLoS One*. 2014;9:e114509. [PubMed: 25489947]
16. Berthier E, Beebe DJ. Lab on a Chip Gradient generation platforms: new directions for an established microfluidic technology. *Lab Chip*. 2014;14:3241–3247. [PubMed: 25008971]
17. Irimia D, Ellett F. Big insights from small volumes: deciphering complex leukocyte behaviors using microfluidics. *J Leukoc Biol*. 2016;100: 291–304. [PubMed: 27194799]
18. Cernada M, Brugada M, Golombek S, Vento M. Ventilator-associated pneumonia in neonatal patients: an update. *Neonatology*. 2014;105:98–107. [PubMed: 24296586]
19. Wilson K, Lewalle A, Fritzsche M, Thorogate R, Duke T, Charras G. Mechanisms of leading edge protrusion in interstitial migration. *Nat Commun*. 2013;4:2896. [PubMed: 24305616]
20. Yoo SK, Lam PY, Eichelberg MR, Zasadil L, Bement WM, Huttenlocher A. The role of microtubules in neutrophil polarity and migration in live zebrafish. *J Cell Sci*. 2012;125:5702–5710. [PubMed: 22992461]
21. Wolf K, Te Lindert M, Krause M, et al. Physical limits of cell migration: control by ECM space and nuclear deformation and tuning by proteolysis and traction force. *J Cell Biol*. 2013;201:1069–1084. [PubMed: 23798731]
22. Wang J, Hossain M, Thanabalasuriar A, Gunzer M, Meininger C, Kubes P. Visualizing the function and fate of neutrophils in sterile injury and repair. *Science*. 2017;358:111–116. [PubMed: 28983053]
23. Albrecht E, Petty HR. Cellular memory: neutrophil orientation reverses during temporally decreasing chemoattractant concentrations. *Proc Natl Acad Sci*. 1998;95:5039–5044. [PubMed: 9560224]
24. Rowat AC, Jaalouk DE, Zwirger M, et al. Nuclear envelope composition determines the ability of neutrophil-type cells to passage through micron-scale constrictions. *J Biol Chem*. 2013;288:8610–8618. [PubMed: 23355469]
25. Stroka KM, Hayenga HN, Aranda-Espinoza H. Human neutrophil cytoskeletal dynamics and contractility actively contribute to transendothelial migration. *PLoS One*. 2013;8:e61377. [PubMed: 23626676]
26. Jacobelli J, Estin Matthews M, Chen S, Krummel MF. Activated T cell trans-endothelial migration relies on Myosin-IIA contractility for squeezing the cell nucleus through endothelial cell barriers. *PLoS One*. 2013;8:e75151. [PubMed: 24069389]
27. Xu J, Wang F, Van Keymeulen A, Rentel M, Bourne HR. Neutrophil microtubules suppress polarity and enhance directional migration. *Proc Natl Acad Sci*. 2005;102:6884–6889. [PubMed: 15860582]
28. Krendel M, Zenke FT, Bokoch GM. Nucleotide exchange factor GEFH1 mediates cross-talk between microtubules and the actin cytoskeleton. *Nat Cell Biol*. 2002;4:294–301. [PubMed: 11912491]
29. Chang YC, Nalbant P, Birkenfeld J, Chang ZF, Bokoch GM. GEF-H1 couples nocodazole-induced microtubule disassembly to cell contractility via RhoA. *Mol Biol Cell*. 2008;19:2147–2153. [PubMed: 18287519]
30. Birukova AA, Smurova K, Birukov KG, et al. Microtubule disassembly induces cytoskeletal remodeling and lung vascular barrier dys-function: role of Rho-dependent mechanisms. *J Cell Physiol*. 2004; 201:55–70. [PubMed: 15281089]
31. Salant DJ, Glover AM, Anderson R, et al. Depressed neutrophil chemo-taxis in patients with chronic renal failure and after renal transplantation. *J Lab Clin Med*. 1976;88:536–545. [PubMed: 787456]
32. Sônego F, Castanheira FV, Ferreira RG, et al. Paradoxical Roles of the Neutrophil in Sepsis: protective and Deleterious. *Front Immunol*. 2016;7:155. [PubMed: 27199981]
33. Brown KA, Brain SD, Pearson JD, Edgeworth JD, Lewis SM, Treacher DF. Neutrophils in development of multiple organ failure in sepsis. *Lancet*. 2006;368:157–169. [PubMed: 16829300]

34. Tavares-Murta BM, Zaparoli M, Ferreira RB, et al. Failure of neutrophil chemotactic function in septic patients. *Crit Care Med.* 2002;30: 1056–1061. [PubMed: 12006803]
35. Shen XF, Cao K, Jiang JP, Guan WX, Du JF. Neutrophil dysregulation during sepsis: an overview and update. *J Cell Mol Med.* 2017;21: 1687–1697. [PubMed: 28244690]
36. Epstein FH, Weiss SJ. Tissue Destruction by Neutrophils. *N Engl J Med.* 1989;320:365–376. [PubMed: 2536474]
37. Arraes SM, Freitas MS, da Silva SV, et al. Impaired neutrophil chemotaxis in sepsis associates with GRK expression and inhibition of actin assembly and tyrosine phosphorylation. *Blood.* 2006;108: 2906–2913. [PubMed: 16849637]

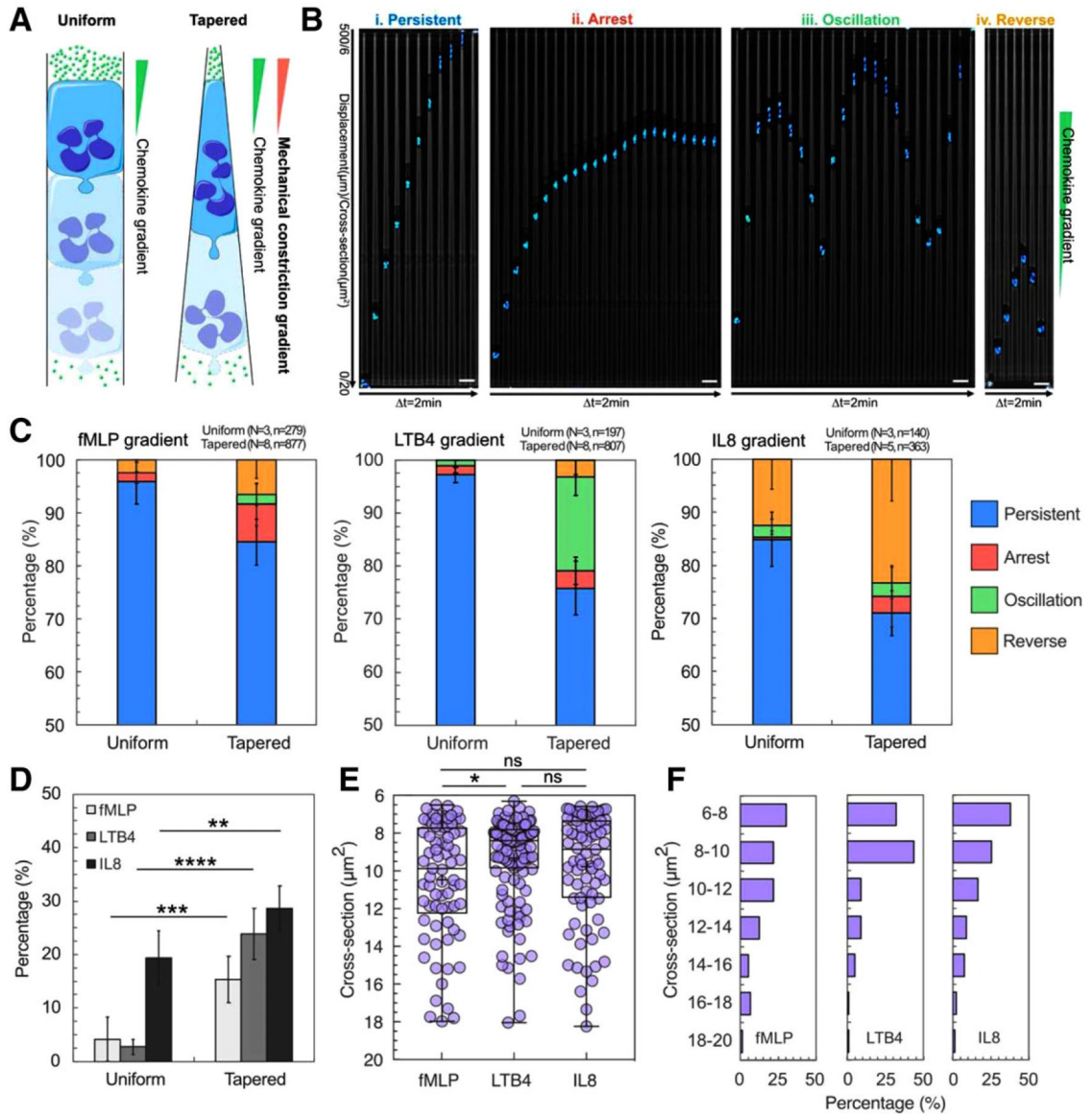


**FIGURE 1. Tapered channels alter neutrophil migration patterns during chemotaxis.**

(A) Schematic illustration of neutrophils migrating in uniform straight channel and tapered straight channel along a chemokine gradient. The neutrophil migrating in tapered channel constantly deforms to adapt to the increasing mechanical constriction. (B) Time-lapse microscopic image array showing the four migration patterns including persistent migration (P), arrest (A), oscillation (O), and retrotaxis (R). The nucleus of neutrophils is stained with Hoechst and pseudo-colored cyan. In each array, the time interval between two images is 2 min. The scale bar is 20  $\mu\text{m}$ . (C) The percentage of each pattern in uniform straight channel and tapered straight channel in chemokine gradients of fMLP, LTB4, and IL8. Percentages of P, A, O, R patterns are presented in blue, red, green, and yellow, respectively, as described in the legend. (D) Comparison of the total percentage of A, O, and R patterns in uniform straight channel and tapered straight channel in chemokine gradients of fMLP, LTB4, and IL8 (\* $P < 0.1$ , \*\*\* $P < 0.001$ , and \*\*\*\* $P < 0.0001$ , two-tailed  $t$ -test). (E) Critical cross-

sections where A, O, and R occur in tapered straight channel in chemokine gradients of fMLP, LTB4, and IL8 (\* $P < 0.1$ , one-way ANOVA).(F) Histograms of A, O, and R critical cross-sections in in chemokine gradients of fMLP, LTB4, and IL8

Author Manuscript

Author Manuscript

Author Manuscript

Author Manuscript

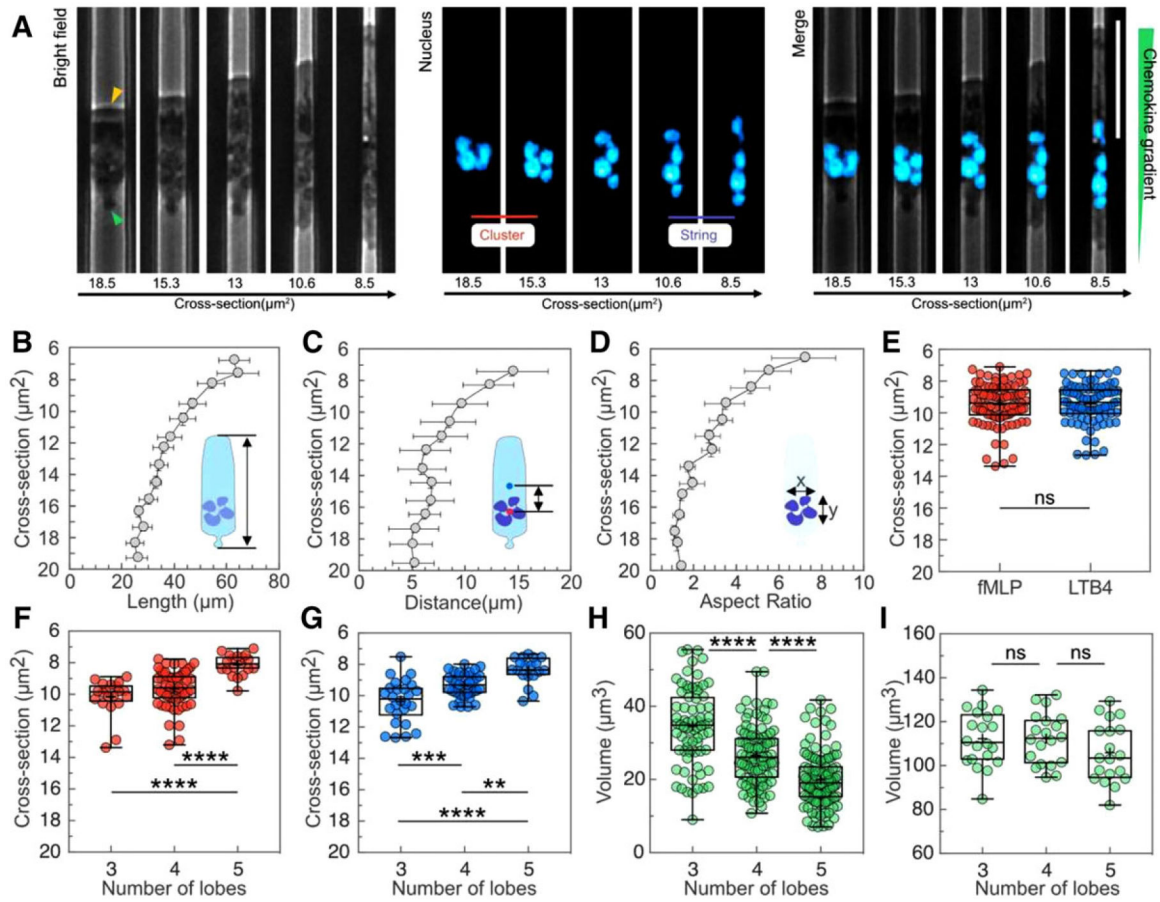


**FIGURE 2. Morphological changes and rearrangement of the nucleus lobes in neutrophils during chemotaxis in tapered channels.**

(A) Phase contrast, fluorescence and overlap of images showing cellular and Nuclear morphology changes during the migration of one typical neutrophil in a channel with cross-section decreasing from  $\sim 19$  to  $\sim 8 \mu\text{m}^2$ . The nucleus of neutrophils was stained with Hoechst and pseudo-colored cyan. The scale bar is  $30 \mu\text{m}$ . The yellow arrow indicates the leading edge. The green arrow indicates the uropod. (B) Cell length increases as the cross-section of the channels decreases ( $n = 15$ ). (C) The distance between the center of the nucleus and the center of the cell over cross-section. (D) The nuclear aspect ratio  $x/y$  over cross-section. (E) The critical cross-sections at which the cluster-string transformation of nuclear lobes occur in gradients of  $100 \text{ nM}$  fMLP or LTB4. The cross-sections at which the cluster-string transformation happens for neutrophils with 3, 4, and 5 lobes in gradients of (F)  $100 \text{ nM}$  fMLP and (G) LTB4 (\*\* $P < 0.01$ , \*\*\* $P < 0.001$ , and \*\*\*\* $P < 0.0001$ , one-way ANOVA). (H) The estimated volume of individual lobes of neutrophils with 3, 4, and 5 lobes (\*\*\*\* $P < 0.0001$ , one-way ANOVA). (I) The total nuclear volume of neutrophils with 3, 4, and 5 lobes

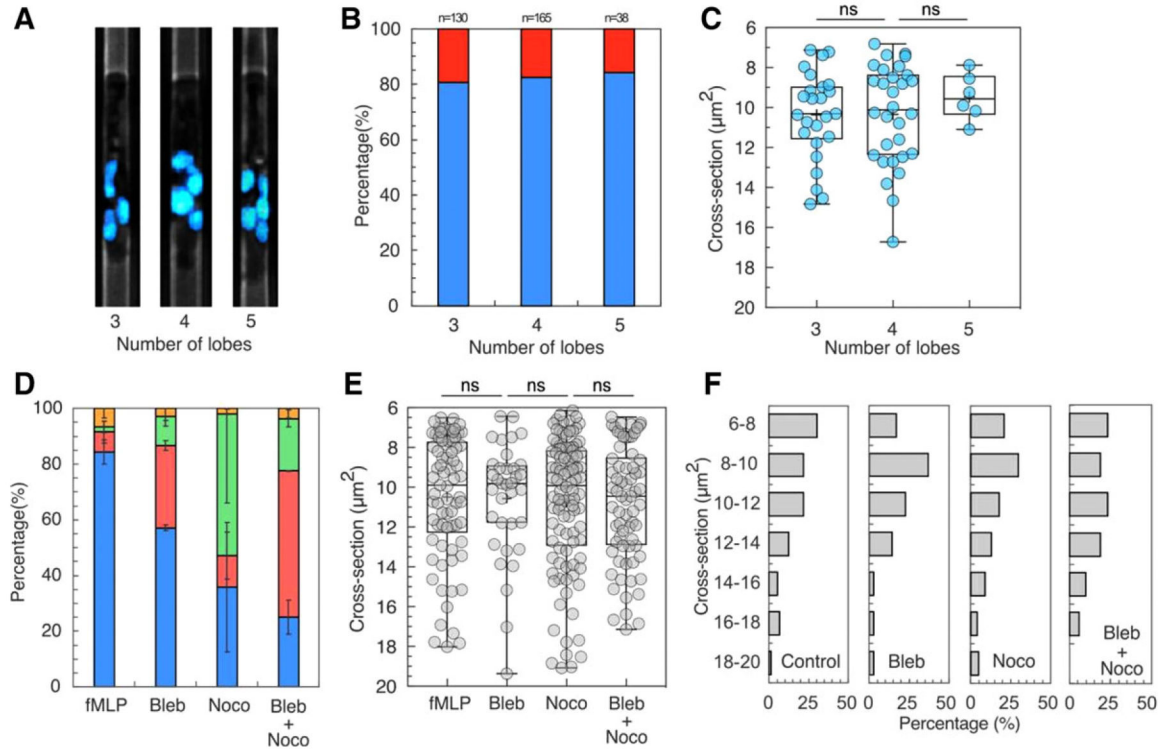


**FIGURE 3. Cellular structures contribute to migration patterns during neutrophil chemotaxis.** (A) Fluorescent microscopic images showing neutrophils with 3, 4, and 5 nuclear lobes. The nucleus is stained with Hoechst and pseudo-colored cyan. (B) The percentage of persistent migration (blue bar) and non-persistent migration (red bar) of neutrophils with 3, 4, and 5 nuclear lobes. (C) Cross-sections at which neutrophils with 3–5 lobes exhibited A, O, and R patterns. (D) The percentage of migration patterns for control and neutrophils treated with actomyosin inhibitor (blebbistatin), microtubule inhibitor (nocodazole), and both inhibitors in fMLP gradient (percentages of P, A, O, R patterns are presented in blue, red, green, and yellow, respectively). (E) The critical cross-sections at which A, O, and R patterns occurred for control and neutrophils treated with blebbistatin, nocodazole, and both inhibitors. (F) Histograms of the critical cross-sections for control, blebbistatin, nocodazole, and combined inhibitor-treated neutrophils



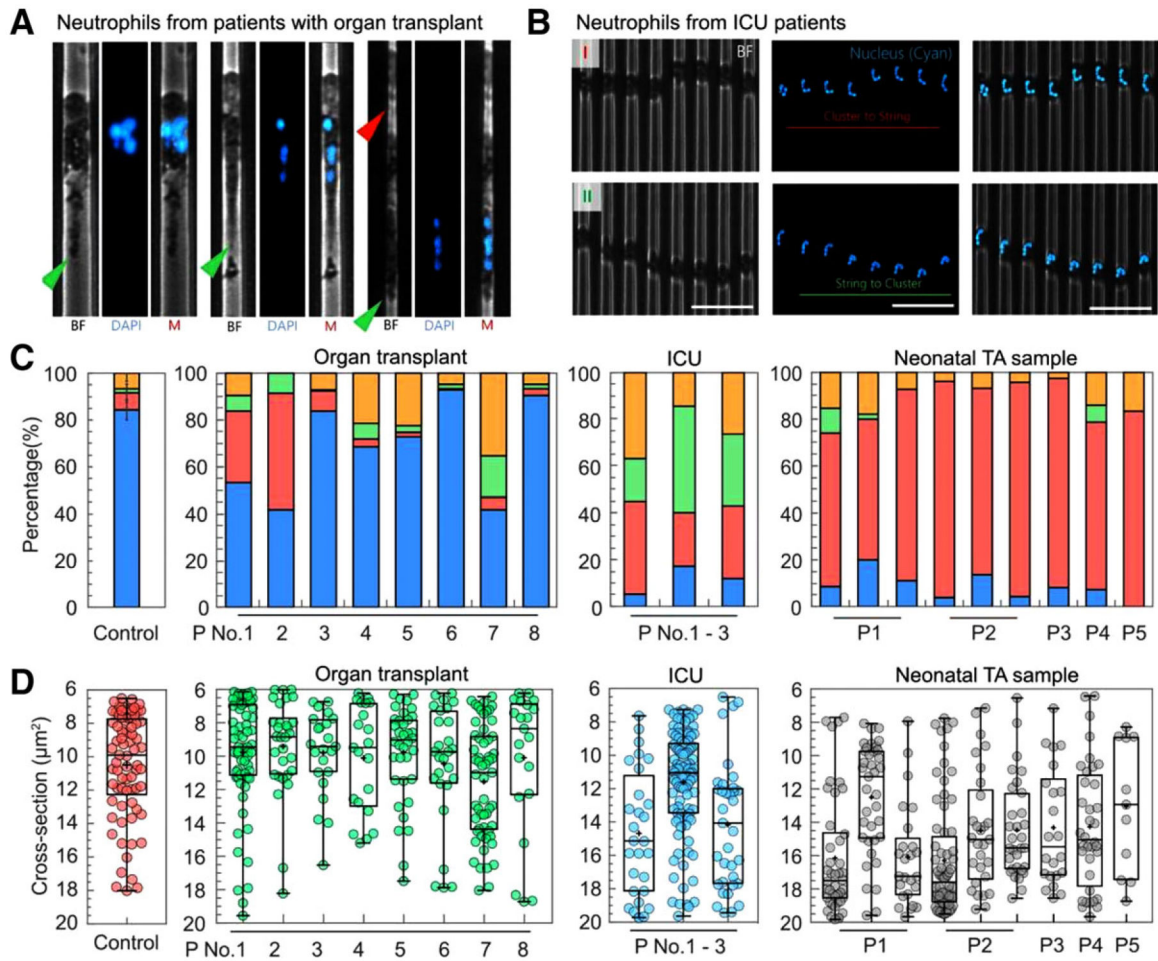


**FIGURE 4. Migration patterns of neutrophils from patients.**

(A) An over-extended leading edge and an elongated tail are common among neutrophils from kidney-transplant patients receiving immune-suppressing treatments. The green arrows indicate the tail of the neutrophil. The red arrow indicates the leading edge of the neutrophil. (B) Nuclear morphology of oscillating neutrophils from ICU patients shows frequent cluster to string to cluster transformation. The scale bar is  $50 \mu\text{m}$ . (C) Larger numbers of neutrophils display arrest, oscillation, and retrotaxis patterns in patients (transplant, ICU, and neonates) compared to the healthy control (percentages of P, A, O, R patterns are presented in blue, red, green, and yellow, respectively). (D) The cross-section for migration patterns transition for neutrophils from transplant patients is comparable to that of controls. The cross-section is significantly larger for ICU patients and neonatal patients